



# Long-Term Variation in Wintertime Atmospheric Diffusion Conditions Over the Sichuan Basin

Guoyin Wang<sup>1,2</sup>, Wennan Leng<sup>3</sup>, Shaojing Jiang<sup>4</sup> and Bangjun Cao<sup>5\*</sup>

<sup>1</sup>Department of Atmospheric and Oceanic Sciences and Institute of Atmospheric Sciences, Fudan University, Shanghai, China,

<sup>2</sup>CMA-FDU Joint Laboratory of Marine Meteorology, Shanghai, China, <sup>3</sup>Gansu Weather Modification Office, Lanzhou, China,

<sup>4</sup>Department of Geography and Spatial Information Techniques, Ningbo University, Ningbo, China, <sup>5</sup>Plateau Atmosphere and Environment Key Laboratory of Sichuan Province, School of Atmospheric Sciences, Chengdu University of Information Technology, Chengdu, China

## OPEN ACCESS

### Edited by:

Longlei Li,  
Cornell University, United States

### Reviewed by:

Pengfei Tian,  
Lanzhou University, China  
Xuanze Zhang,  
Institute of Geographic Sciences and  
Natural Resources Research (CAS),  
China  
Qinjian Jin,  
University of Kansas, United States

### \*Correspondence:

Bangjun Cao  
caobj1989@163.com

### Specialty section:

This article was submitted to  
Atmosphere and Climate,  
a section of the journal  
Frontiers in Environmental Science

**Received:** 24 August 2021

**Accepted:** 27 October 2021

**Published:** 10 November 2021

### Citation:

Wang G, Leng W, Jiang S and Cao B  
(2021) Long-Term Variation in  
Wintertime Atmospheric Diffusion  
Conditions Over the Sichuan Basin.  
*Front. Environ. Sci.* 9:763504.  
doi: 10.3389/fenvs.2021.763504

Atmospheric diffusion is one of the factors affecting local air quality, dominating the evolution of air pollution episodes. Previous work has emphasized the unfavorable diffusion conditions in the Sichuan Basin resulting from its complex terrain. However, the recent spatiotemporal variation in atmospheric diffusion conditions in the basin and their effects on local air quality remain unclear. Based on the wind speed, boundary layer height, vertical potential temperature difference of ERA5 analysis, two independent metrics containing information on horizontal and vertical diffusion ability, i.e., ventilation coefficient ( $V_E$ ) and the air stagnant conditions (ASI), are involved to indicate wintertime atmospheric diffusion conditions in the basin. Both  $V_E$  and ASI reveal a decrease tendency of atmospheric diffusion condition from the northwestern portion of the basin to the southeast. In terms of the long-term variation in diffusion conditions,  $V_E$  showed a broader increasing trend from 1979 to 2019, with a distinct increase in the western region. In contrast, the occurrence of air stagnation events has declined  $-3\sim-6\%$ /decade in the basin, more significantly over the western basin. Both the increase in  $V_E$  and the decrease in air stagnation frequency indicate the improvement of atmospheric diffusion conditions in the Sichuan Basin from 1979 to 2019, which mitigates the effects of air pollutant emissions to some extent. The enhancement of diffusion conditions is due to the improvement of vertical diffusion conditions. The lowest seasonal PM<sub>2.5</sub> concentrations occur in the northwestern basin, where  $V_E$  is highest and ASI is lowest. Atmospheric diffusion conditions can explain approximately 25–50% of the interannual variation in PM<sub>2.5</sub> concentrations in Chengdu.

**Keywords:** atmospheric diffusion ability, ventilation coefficient, atmospheric boundary layer, air pollution, Sichuan Basin

## 1 INTRODUCTION

Severe and frequent air pollution has become a major environmental concern in China in recent years (Dang and Liao, 2019; Hu et al., 2019; Li et al., 2019; Mu and Zhang, 2014). Pollution episodes, characterized by dense fine particles and low horizontal visibility, have many negative impacts on transportation, public health and weather/climate (Che et al., 2019; Chen H. et al., 2019; Chen S. et al., 2019; Feng and Wang, 2019; He Y. et al., 2018; Jian et al., 2018; Wang et al., 2009; Wang et al.,

2018b). Numerous studies have been conducted to reveal the mechanisms of haze formation and its long-term variation, indicating that high pollutant emissions and unfavorable meteorological conditions are two key factors (Chen et al., 2018; Ding et al., 2019; Fan et al., 2020; Huang et al., 2018; Miao et al., 2017; Hu et al., 2021). Secondary aerosol formation also contributes to the explosive growth of particulate concentrations, especially during the developing stage of each pollution episode (Guo et al., 2019; He J. et al., 2018; Ma et al., 2020; Sun et al., 2013; Zhao D. et al., 2018). Moreover, variation in East Asian winter monsoon strength, El Niño-Southern Oscillation, Arctic Sea ice extent and the phase of Pacific Decadal Oscillation change background atmospheric circulation and in turn affect the formation of air pollution at different time scales (Cai et al., 2017; Chang et al., 2020; Chen and Wang, 2015; Li et al., 2016; Wang et al., 2020; Yin et al., 2017).

There are four main regions suffering from the severe air pollution in China: the North China Plain (NCP), Yangtze River Delta (YRD), Pearl River Delta (PRD) and Sichuan Basin (Bi et al., 2016; Wang and Zhang, 2020a; Wang and Zhang, 2020b; Xia et al., 2020; Zhang and Geng, 2019; Zhao and Garrett, 2015; Zhao et al., 2020). Compared to the first three mega-regions, less attention has been given to the air quality in the Sichuan Basin, especially the long-term variation in air quality and its attribution in terms of the long-term variation. The Sichuan Basin comprises the greater part of eastern Sichuan Province and the western portion of Chongqing municipality located in southwestern China. It is surrounded by the highlands of the Tibetan Plateau to the west, the YunGui Plateau to the south, the Wu Mountains to the east and the Daba Mountains to the north (Cao et al., 2020; Liu et al., 2021; Zhong et al., 2019). The complex local topography stimulates special meteorological conditions with lower surface wind, higher relative humidity and a stable boundary layer, which is conducive to the formation of haze in the basin (Liao et al., 2018; Ning et al., 2018). Therefore, although the anthropogenic emissions in the basin are not as much as those in the other three regions, its air pollution ranks in the top four regions in China (Fan et al., 2015; Gui et al., 2019; Liu et al., 2019; Zhang et al., 2019; Zhao S. et al., 2018).

Emissions in a specific region do not normally change much over a short period, but local meteorological patterns change rapidly and can strongly affect the accumulation, removal, and transport of air pollutants and thus the day-to-day variation in air pollutants (Chen et al., 2020; Zhang, 2017; Zhang et al., 2014; Zhao C. et al., 2018). A combined metric to evaluate the effects of atmospheric conditions on air pollution is the atmospheric diffusion ability, which cannot be ignored in the quantitative evaluation of historical emission reduction effects and the development of emission reduction measures. The atmospheric ventilation coefficient ( $V_E$ ) provides an indication of the ability of the atmosphere to disperse pollutants over a region and is the metric most frequently used to predict the evolution of local diffusion conditions. Generally,  $V_E$  in the basin is relatively weak due to special terrain (Ning et al., 2019; Tang et al., 2015; Zhu et al., 2018). Severe air pollution episodes are also linked to the occurrence of air stagnation conditions (Wang et al., 2016). A previous work highlighted that the Sichuan Basin experiences

frequent air stagnation conditions for approximately half of the whole year, which is the worst atmospheric diffusion condition among the four severely polluted regions in China listed above. However, the work of Wang et al. (2016) has only provided an average frequency of air stagnation in the basin based on the meteorological conditions at several PM<sub>2.5</sub> observation stations from 2013 to 2017. The thresholds for the occurrence of air stagnation events are established according to the global air pollutant concentrations, which may smooth some local air pollution information. In addition, the spatial variation in the occurrence frequency of air stagnation conditions in the basin, how atmospheric diffusion conditions have changed in recent decades, and the extent of impact of temporal and spatial variation in atmospheric diffusion conditions on local air quality remain unclear.

In this work, the long-term variation in  $V_E$  and the occurrence of air stagnation events are examined to investigate the spatial and temporal variation in atmospheric diffusion conditions in the Sichuan Basin. The regional thresholds for air stagnation conditions are defined in **Section 2**. Spatiotemporal variation in diffusion conditions and their effects on local air quality are shown in **Section 3**.

## 2 DATA AND METHOD

### 2.1 Data

**Figure 1** shows the altitude distribution around the Sichuan Basin. Sixty-four air quality observation stations from the Ministry of Ecology and Environment of the People's Republic of China are located in the basin (i.e., altitude under 1,000 m). The 64 stations belong to 14 cities in Sichuan Province and Chongqing City. The PM<sub>2.5</sub> concentrations observed from December 2013 to December 2019 at the 64 stations were used to indicate the variation in ambient air quality. The fifth-generation European Centre for Medium-Range Weather Forecasts atmospheric reanalysis data (ECMWF ERA5) with a horizontal resolution of 0.25°×0.25° from 1979 to 2019 were used to supply meteorological variables for the Sichuan Basin. The evaluation of the representation and accuracy of ERA5 over Sichuan Basin are shown in SI. The mean wind speeds at 1,000, 925, 900, 875 and 850 hPa (Wind\_BL) are considered the average wind speeds in the boundary layer. The 10-m wind speed (Wind\_10), potential temperature difference between 925 hPa and 850 hPa ( $\Delta\theta$ ), boundary layer height (BLH), and total precipitation were incorporated to evaluate the atmospheric diffusion conditions in the Sichuan Basin. ERA5 BLH is diagnosed as the height where the bulk Richardson number becomes superior to 0.25 (<https://apps.ecmwf.int/codes/grib/param-db?id=159>). Given the relatively poor performance for the stable boundary layer in model simulation (Stull, 2012), only the 14:00 local time (6:00 UTC) air quality and meteorological dataset were used in this work. The altitude distribution around the Sichuan Basin was derived from the global digital elevation model (DEM), with a horizontal grid spacing of 30 arc seconds (approximately 1 km).

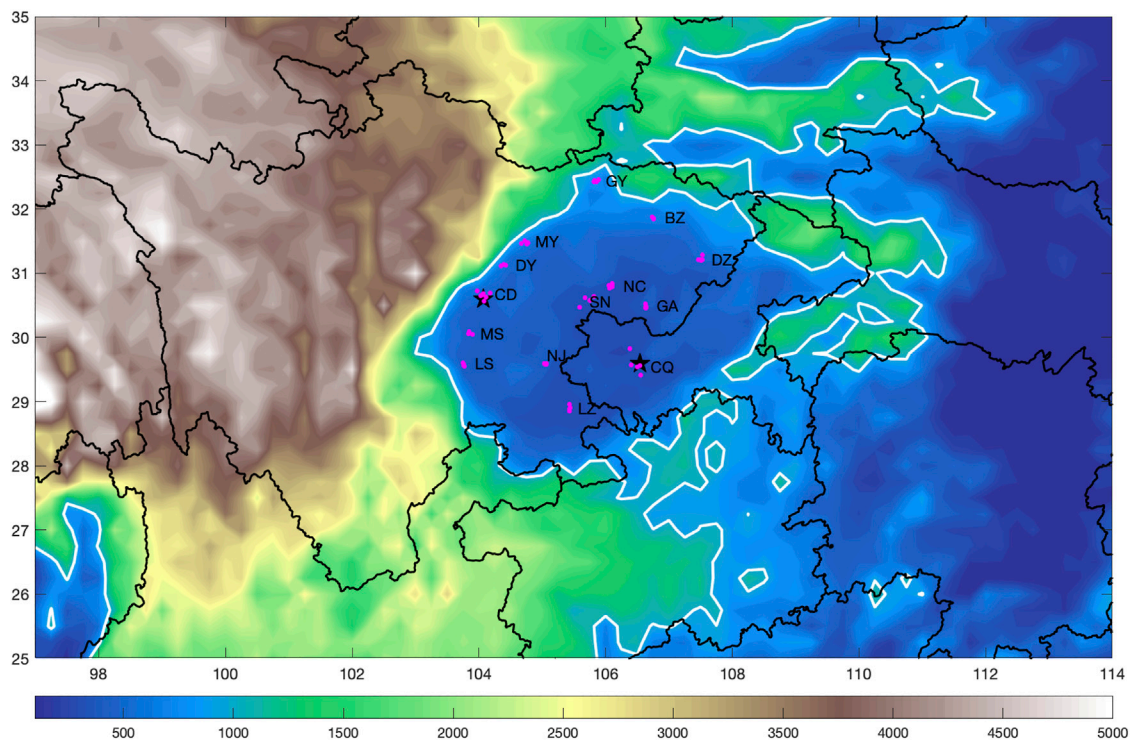


**FIGURE 1** | Spatial distribution of elevation around the Sichuan Basin (unit: m) and 64 air quality observation stations in the basin. The edge of the Sichuan Basin is marked by the 1000-m contour line (white line). Magenta dots indicate the locations of the 64 air quality stations. GY (Guangyuan), BZ (Bazhong), MY (Mianyang), DY (Deyang), CD (Chengdu), MS (Meishan), LS (Leshan), NC (Nanchong), SN (Suining), NJ (Nenjiang), DZ (Dazhou), GA (Guang'an), CQ (Chongqing), and LZ (Luzhou) indicate the 14 cities in the basin. CD and CQ are marked by black stars.

## 2.2 Method for Calculating the Ventilation Coefficient ( $V_E$ ) and Air Stagnation Index (ASI)

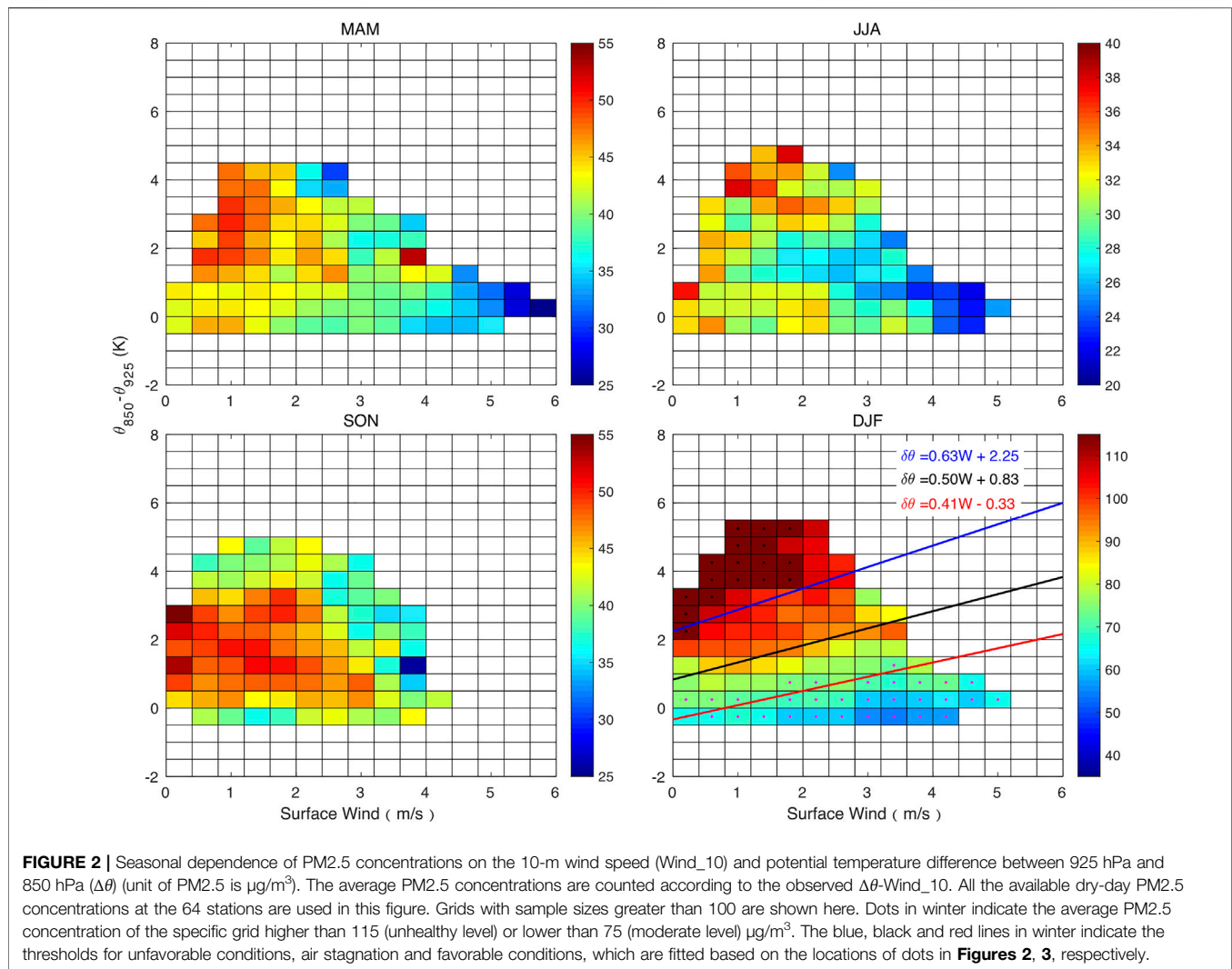
The ventilation coefficient ( $V_E$ ) is a product of the boundary layer height and average vertical wind speed through the boundary layer. The higher the  $V_E$  is, the more efficiently the atmosphere can disperse near-surface pollutants and the better the air quality. The  $V_E$  can be calculated by (Lu et al., 2012; Liu et al., 2012; Sujatha et al., 2016):

$$V_E = \int_0^{BLH} u(z) dz = \overline{u_{BL}} \cdot BLH$$

where  $\overline{u_{BL}}$  is the average wind speed in the boundary layer.

Air stagnation is considered to consist of light winds so that horizontal dispersion is at a minimum, a stable lower atmosphere that effectively prevents vertical escape, and no precipitation to wash any pollution away (Wang et al., 2018a). Severe air pollution episodes are usually related to the presence of air stagnation. There exist several types of quantitative definitions for air stagnation events based on different meteorological variables depending on the domain concerned. Previous work has shown relatively high frequency of air stagnation events in the Sichuan Basin based on a nationwide unified air stagnation

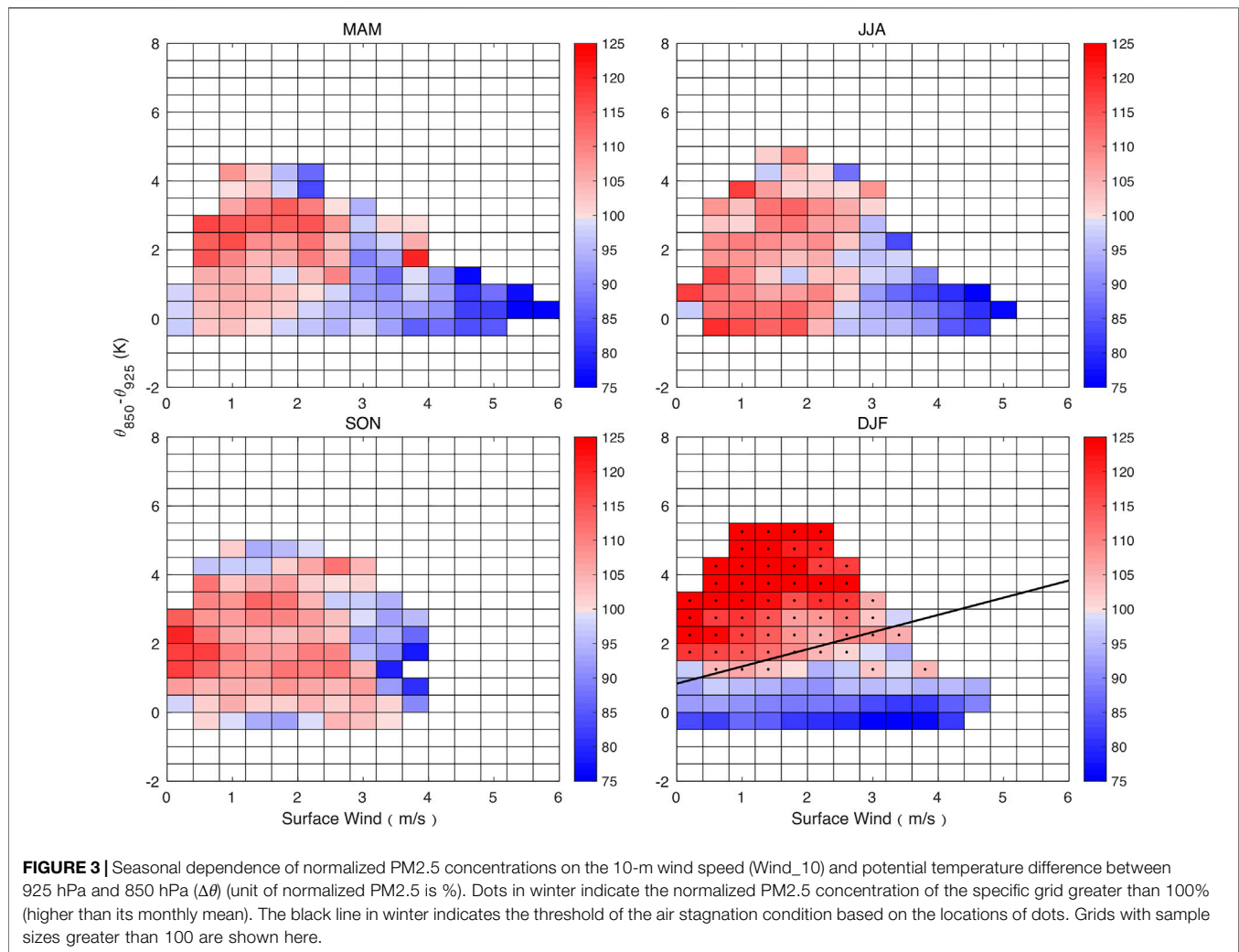
threshold. However, it is essential to identify a more regionally applicable air stagnation definition due to the complicated terrain around the basin. Here, the 10 m (Wind<sub>10</sub>) wind speed and potential temperature difference between 925 hPa and 850 hPa ( $\Delta\theta$ ) were used to measure the atmospheric horizontal and vertical dispersion capability (Wang et al., 2016; Wang et al., 2018a). Higher  $\Delta\theta$  means stronger temperature inversion in the low troposphere, which indicates lower capability of vertical diffusion and implies higher concentration of surface PM<sub>2.5</sub>. In terms of the surface wind speed, a higher wind speed indicates more effective outward transport of local air pollutants. Both vertical and horizontal diffusion control the variation in surface PM<sub>2.5</sub> concentrations. However, how do Wind<sub>10</sub> and  $\Delta\theta$  coordinate to manage the diffusion of air pollutants? **Figure 2** shows the seasonal average PM<sub>2.5</sub> concentrations corresponding to the specific Wind<sub>10</sub> and ( $\Delta\theta$ ) ranges. Dry-day PM<sub>2.5</sub> concentrations at the 64 stations were used to identify the threshold of air stagnation. Generally, PM<sub>2.5</sub> concentrations decrease with increasing wind speeds and increase with increasing  $\Delta\theta$ , especially in spring and winter. PM<sub>2.5</sub> concentrations are the most sensitive to the variation in Wind<sub>10</sub> and  $\Delta\theta$  in winter, with PM<sub>2.5</sub> concentrations exceeding 110  $\mu\text{g}/\text{m}^3$  under the conditions of high- $\Delta\theta$  and low-Wind<sub>10</sub> compared to values lower than 50  $\mu\text{g}/\text{m}^3$  for the situations of low- $\Delta\theta$  and high-Wind<sub>10</sub>. Therefore, we only focus



on the wintertime atmospheric diffusion conditions hereafter. Taking the  $\Delta\theta$ -Wind<sub>10</sub> locations with PM2.5 concentrations lower than 75 (moderate level) or higher than 115  $\mu\text{g}/\text{m}^3$  (unhealthy level) as the conditions favorable or unfavorable, respectively, for air pollutant diffusion, **Figure 2** shows the  $\Delta\theta$ -Wind<sub>10</sub> thresholds for favorable and unfavorable conditions in winter. If the observed  $\Delta\theta$ -Wind<sub>10</sub> values in a region exceed the unfavorable threshold, the atmospheric diffusion condition for the specific day is considered unfavorable. Similarly, if  $\Delta\theta$ -Wind<sub>10</sub> meets the criterion of less than the favorable threshold, conditions are defined as favorable.

To eliminate the effects of seasonal, spatial, and long-term variations in PM2.5 concentration, PM2.5 concentrations on dry days were normalized by their corresponding monthly mean values. That is, if the normalized PM2.5 concentrations exceeded 100%, the original PM2.5 concentrations were higher than their monthly mean, and the corresponding atmospheric conditions were defined as air stagnation conditions. **Figure 3**

displays the relationship between normalized PM2.5 concentrations and the variation in  $\Delta\theta$ -Wind<sub>10</sub>. It shows the same distribution pattern for normalized PM2.5 concentrations as that of the original PM2.5 concentrations; i.e., with decreasing  $\Delta\theta$  and increasing Wind<sub>10</sub>, normalized concentrations tend to decrease. **Figure 3** shows the fitting line of the threshold of the air stagnation condition (i.e., 100% normalized concentrations) in winter. If the observed  $\Delta\theta$ -Wind<sub>10</sub> is located in the upper region of the fitting line, the atmospheric conditions will be defined as air stagnation conditions. Therefore, unfavorable conditions are somewhat extreme and severe air stagnation conditions. It is assumed that all rainy days with 4-h precipitation amounts higher than 0.5 mm are by default no-air-stagnation days because of wet deposition. If precipitation exceeds 1 mm, the atmospheric conditions are considered favorable due to the more effective wet deposition. A day can be classified as an air-stagnation or no-air-stagnation day based on the observed  $\Delta\theta$ -Wind<sub>10</sub>. The monthly or seasonal occurrence of air stagnation days is defined



as the air stagnation index (ASI), which combines the horizontal and vertical atmospheric diffusion conditions.

### 3 RESULTS

#### 3.1 Distribution of the Climatology of Atmospheric Diffusion Conditions in the Sichuan Basin

The wintertime climatology distributions of  $V_E$ , and frequencies of ASI, favorable and unfavorable conditions over the Sichuan Basin are shown in **Figure 4**.  $V_E$  tended to decrease from the northwest region of the basin to the southeast, with the maximum  $V_E$  exceeding  $3,400 \text{ m}^2/\text{s}$  compared to the lowest value of approximately  $1,600 \text{ m}^2/\text{s}$ . **Figure 5** shows the distribution of Wind<sub>BL</sub> and BLH, which are used for the calculation of  $V_E$ . The BLH and average wind speed in the boundary layer were higher in the northwest portion of the basin, where the elevations are in the range of 500–1,000 m (**Figure 1**). The sloped terrain in the

northwest area of the basin may increase absorption of solar radiation (Wang and Wang, 2015), enhancing the development of the daytime convective boundary layer and the downward transport of upper momentum, which leads to higher BLH and Wind<sub>BL</sub>. In addition, the northwestern region of the basin is also a principal track of northwestern cold air to the basin, and the airflow over the northern mountain brings cold air and heavy wind to the northwestern basin. Deeper in the basin, where the elevation is lower than 500 m, both BLH and average wind speed declined by approximately 40% compared to the northwest region due to the blocking of terrain and the effect of valleys. The almost synchronous spatial variations in BLH and Wind<sub>BL</sub> contributed to the evident regional difference in  $V_E$  in the basin.

As a metric combining the atmospheric horizontal and vertical diffusion conditions and wet deposition effect, the frequency of ASI can be used to measure the local atmospheric diffusion capacity more comprehensively. **Figure 4** shows an almost opposite spatial distribution of ASI to  $V_E$  over the basin, with an increasing tendency from the northwest to the southeast region. The spatial distribution pattern of ASI frequency

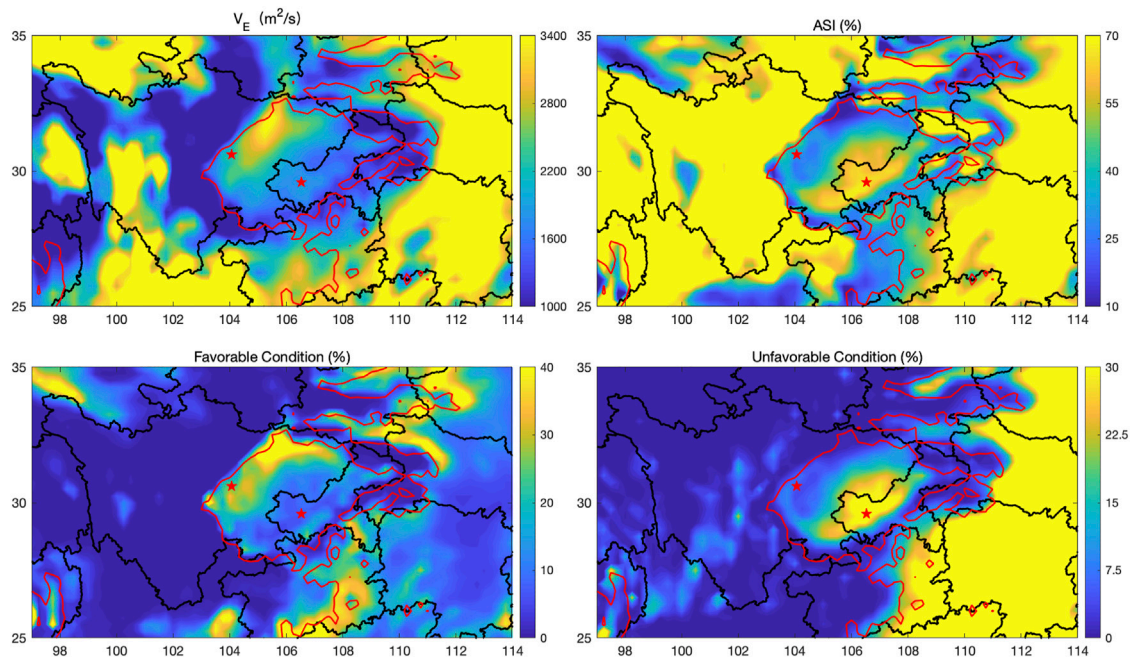


**FIGURE 4** | Distributions of ventilation coefficient ( $V_E$ ), frequency of air stagnation index (ASI), favorable condition and unfavorable condition during the winters from 1979 to 2019 in Sichuan Basin. Two red pentagrams indicate the locations of Chengdu and Chongqing.

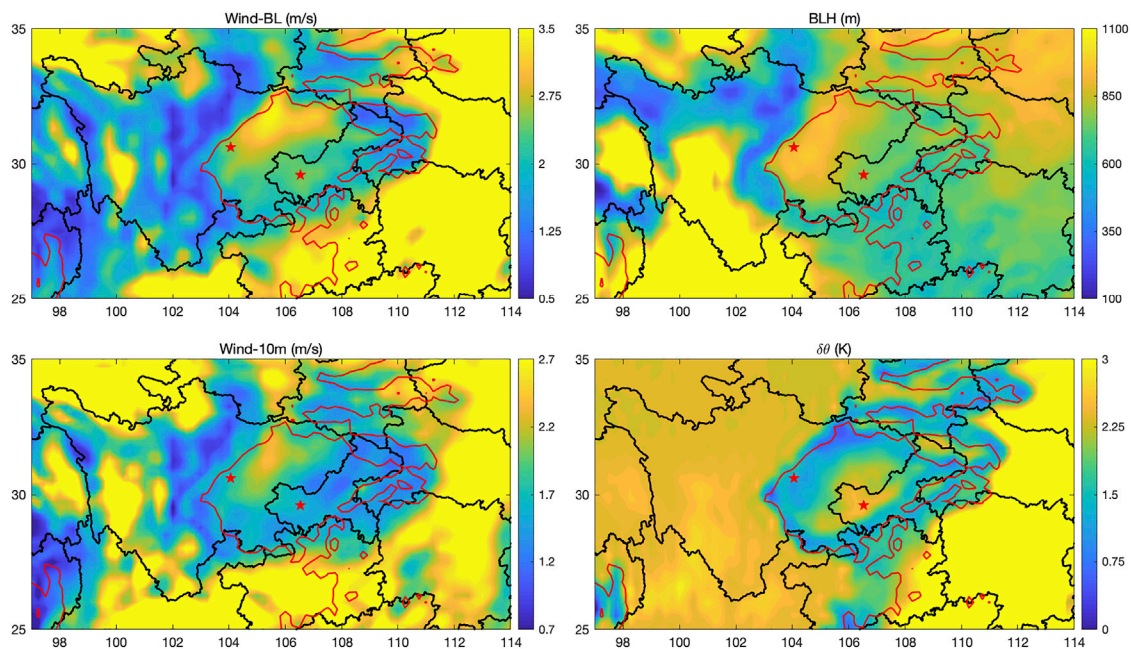


**FIGURE 5** | Distributions of boundary layer wind speed (Wind-Bl), boundary layer height (BLH), 10-m wind speed (Wind-10m) and potential temperature difference between 925 hPa and 850 hPa ( $\Delta\theta$ ) during the winters from 1979 to 2019 in the Sichuan Basin. Two red pentagrams indicate the locations of Chengdu and Chongqing.

climatology over the basin agrees well with the previous work (Liao et al., 2018). The wintertime ASI frequency was lower than 20% in the northwestern part of the basin, while it increased to over 60% in the southeastern low-altitude region. The spatial

correlation coefficient between ASI frequency and elevation was -0.44 over the basin region, indicating that more frequent air stagnation events occurred in the low-altitude region. According to the climatology of the surface wind speed (Wind-10) and

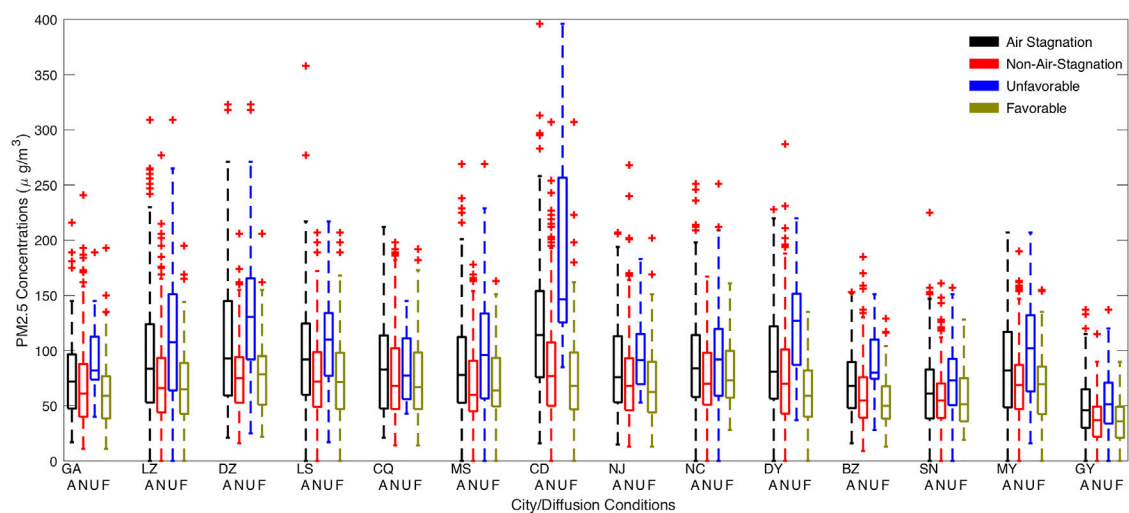


**FIGURE 6** | Box plot of daily mean PM<sub>2.5</sub> concentrations according to different metrics of atmospheric diffusion conditions in the specific cities. Abbreviations of the 14 cities are the same as in **Figure 1**. Labels of A/N/U/F in the X-axis indicate air stagnation, no-air-stagnation days, and unfavorable and favorable conditions, respectively.

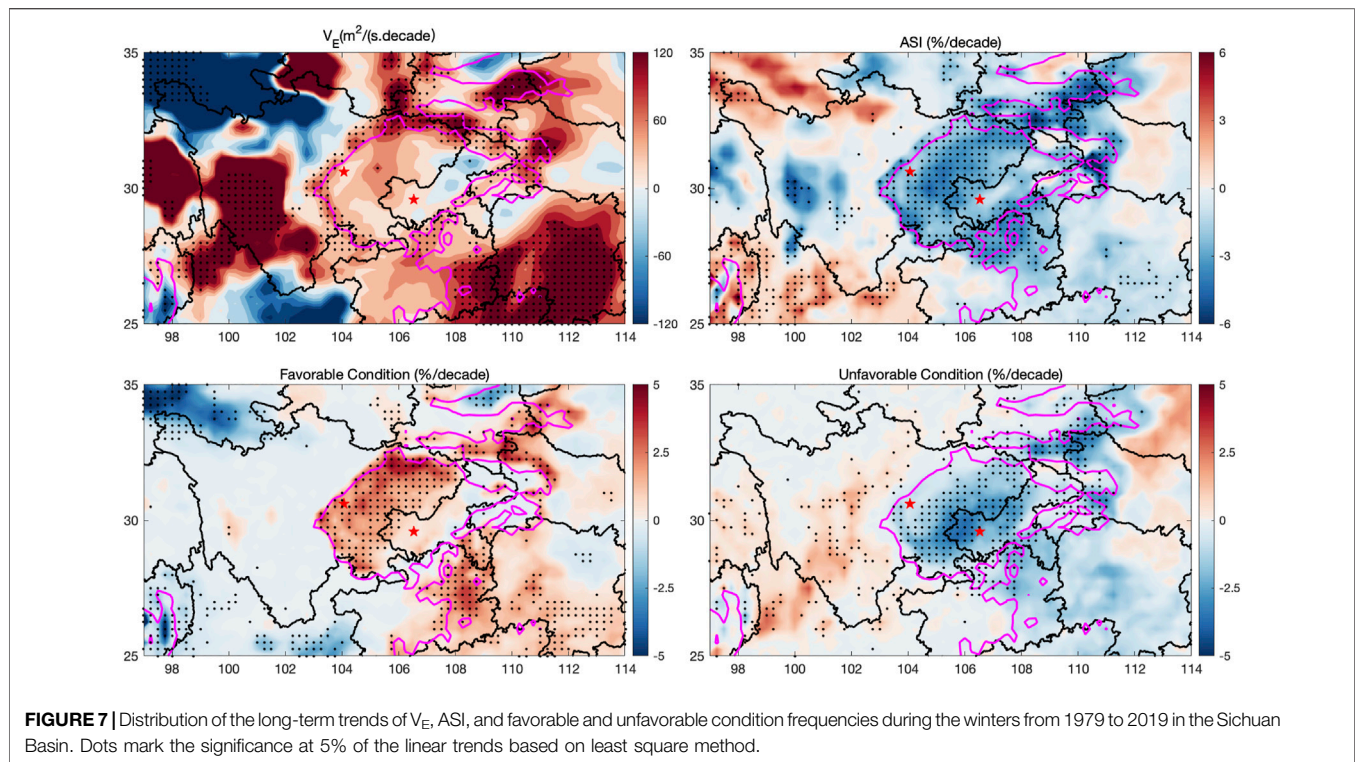
potential temperature difference between 925 hPa and 850 hPa ( $\Delta\theta$ ) in **Figure 5**, Wind<sub>10</sub> showed a decreasing tendency from the northwest to the southeast region, similar to the distribution of Wind<sub>BL</sub>. In the vertical direction,  $\Delta\theta$  was lower in the southeast low-altitude region and higher in the northwest region, in contrast to the distribution of BLH. Based on the definition of ASI, low wind<sub>10</sub> simultaneous with high  $\Delta\theta$  indicates a condition suitable for the occurrence of air stagnation. The consistent distribution of horizontal and vertical diffusion capability in space led to the spatial differences in ASI frequency over the basin.

A day can be defined as an air-stagnation day or a no-air-stagnation day, based on the threshold of  $\Delta\theta$ -Wind<sub>10</sub> in **Figure 3**. In general, the capability for air pollutant diffusion was higher on no-air-stagnation days than on air-stagnation days. However, **Figure 6** shows a large range of observed PM<sub>2.5</sub> concentrations on air-stagnation days and on no-air-stagnation days, which indicates that the occurrence of air stagnation is not sufficiently accurate to measure the atmospheric diffusion ability of air pollutants. Applying the thresholds of national air quality standards, the  $\Delta\theta$ -Wind<sub>10</sub> relationship corresponding to moderate ( $75 \mu\text{g}/\text{m}^3$ ) and unhealthy ( $115 \mu\text{g}/\text{m}^3$ ) air quality levels is used to represent very favorable and very unfavorable diffusion conditions. **Figure 6** shows a clearer distinction PM<sub>2.5</sub> concentrations between favorable and unfavorable than that for air-stagnation and no-air-stagnation days, demonstrating a more rational measurement of atmospheric diffusion conditions based on the occurrence of favorable and unfavorable conditions. According to the distribution of favorable and unfavorable condition frequencies in **Figure 4**, more than 40% of favorable diffusion conditions occurred in the northwestern part of the basin, compared to less than 10% for unfavorable conditions. In the southeastern low-altitude region of the basin, the frequency of

favorable conditions decreased to approximately 15%, and the occurrence of unfavorable conditions exceeded 30%. Because unfavorable conditions are extreme air stagnation conditions, the spatial distribution pattern of occurrence frequencies was almost identical, with an overall lower frequency of unfavorable conditions. The high frequency of unfavorable diffusion conditions in the southeastern region of the basin exacerbates local wintertime air quality.

### 3.2 Long-Term Variation in Atmospheric Diffusion Conditions in the Basin

The emission of air pollutants and their precursors is the initial cause of air pollution episodes, but the daily fluctuations and evolution of air quality are exacerbated by unfavorable meteorological conditions, which can be measured based on atmospheric diffusion conditions. Air pollutant emissions are thought to have increased due to anthropogenic activities in recent decades, which is the main reason for the worsening of ambient air quality. However, it remains unclear how the recent atmospheric diffusion conditions changed and what the effect of atmospheric condition variation on the air quality is. **Figure 7** shows the patterns of variation in wintertime atmospheric diffusion conditions in the basin during the period of 1979–2019. The linear trends of  $V_E$ , ASI frequency, and favorable and unfavorable condition frequencies indicate the variation in atmospheric diffusion conditions. In general,  $V_E$  showed a broadly increasing trend in the Sichuan Basin from 1979 to 2019, with a higher positive tendency in the western region and a weak negative trend in the eastern part. The  $V_E$  in Chengdu and Chongqing cities showed an almost identical weakly positive tendency of approximately  $20 \text{ m}^2/(\text{s decade})$ . Although the linear trend was insignificant, the consistent increase in  $V_E$  in the basin represents an improvement in

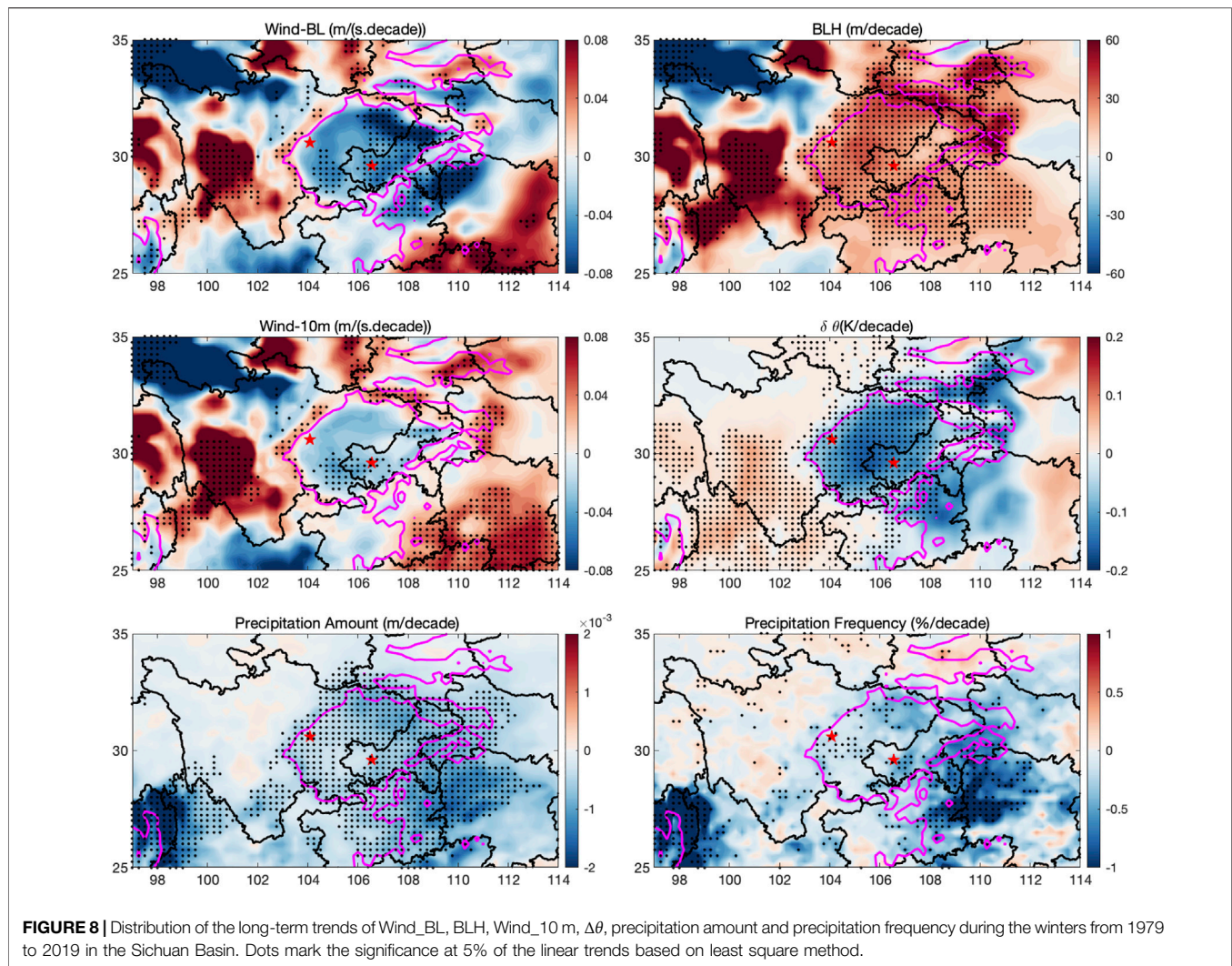


atmospheric diffusion conditions in recent decades, which may alleviate to a certain extent the increase in anthropogenic emissions. The temporal variation of the two factors affecting  $V_E$  are shown in **Figure 8**. The wind speed in the boundary layer reveals a decreasing trend in the basin, with a significant negative trend in the eastern part, where the Wind\_BL was lower than that in the northwestern region. That is, the already weak horizontal diffusion conditions decreased further. However, in the vertical direction, a significant increase in BLH occurred over most regions of the basin, which in part counteracts the effects of the decreasing Wind\_BL and resulted in an overall increase in  $V_E$ .

Measuring the variation in diffusion conditions from another view, **Figure 7** also shows the pattern for the ASI frequency. Contrary to the increasing  $V_E$  tendency, the wintertime occurrence of air stagnation events exhibited a decreasing trend of  $\sim 3\text{--}6\%$ /decade in the basin. The negative tendency of the ASI frequency was more significant over the western part of the basin than in the eastern region, which is similar to the pattern for  $V_E$ . A lower frequency of ASI also implies better atmospheric diffusion conditions. The variation in surface wind speed was not significant in the basin as shown in **Figure 8**. For wet deposition, precipitation frequency is considered as the main factor based on the definition of ASI. The variation in precipitation frequency was weak and insignificant, although the wintertime precipitation amount showed a significant decreasing trend during the study period. Therefore, the impact of horizontal diffusion conditions and wet deposition on ASI variation can be neglected, and the decreasing trend in ASI frequency was driven by the negative tendency of  $\Delta\theta$ . In sum, regardless of the increase in  $V_E$  or the decrease in ASI frequency, the two independent metrics exhibit

improvements in atmospheric diffusion conditions in the Sichuan Basin from 1979 to 2019, which mitigates the effects of air pollutant emissions to some extent. Given the causes underlying variation in  $V_E$  and ASI, it is the recent better vertical diffusion conditions (i.e., higher BLH and weaker  $\Delta\theta$ ) that have contributed to the overall improvement of atmospheric diffusion conditions.

The variation in frequencies of favorable and unfavorable conditions is also illustrated in **Figure 7**. **Figure 7** shows a large area of increasing frequency of favorable conditions in the basin, which indicates the improvement in atmospheric diffusion conditions. The occurrence of favorable conditions increased significantly by  $4\text{--}5\%$ /decade over the western part of the basin, but the tendency was not significant in the eastern region. The spatial distribution of variation in frequency of favorable conditions was consistent with that for  $V_E$ . The higher the  $V_E$  and favorable condition frequency, the better the diffusion conditions. Both  $V_E$  and favorable condition frequency indicated remarkable improvement in diffusion conditions over the western area of the basin, where the atmospheric diffusion conditions were better than in other regions. For unfavorable conditions, which are highly likely to exacerbate severe air pollution, the frequency showed a significant falling trend from 1979 to 2019 over the southeast low-altitude region. Although the increasing tendency of favorable condition frequency was not remarkable over the southeast low-altitude region, the significant decrease in the occurrence of unfavorable conditions marks an improvement in the local atmospheric diffusion conditions. Overall, a higher frequency of favorable diffusion conditions occurred over the



western better-diffusion region, and a lower frequency of unfavorable diffusion conditions took place over the eastern worse-diffusion region; both processes noticeably enhanced the atmospheric diffusion ability.

### 3.3 Effects of Atmospheric Diffusion Conditions on Air Quality

If the air pollutant emissions are identical for all cities, the differences in ambient air pollutant concentrations are almost determined by atmospheric diffusion conditions; i.e., better diffusion ability corresponds to low air pollutant concentrations, and vice versa. **Figure 9** shows the winter average PM<sub>2.5</sub> concentrations varying with atmospheric diffusion conditions in the 14 cities within the basin. The cities are presented in ascending order of average  $V_E$ , with the lowest  $V_E$  in Guang'an (GA) and the highest value in Guangyuan (GY). Similar to the spatial distribution in **Figure 4**, **Figure 9** shows decreasing trends of ASI and unfavorable condition

frequencies with increasing in  $V_E$ . Generally, average winter PM<sub>2.5</sub> concentrations decline with increasing local atmospheric diffusion conditions. Guangyuan has the best air quality due to its excellent atmospheric diffusion ability. However, the atmospheric diffusion conditions are moderate in Chengdu (CD), which is the capital of Sichuan Province, and its air pollution is the most serious among the 14 cities. Located in the northwestern part of the basin, Mianyang (MY) has the second highest  $V_E$ , but its air quality is worse than in the other cities with approximately the same level of  $V_E$ . Chengdu and Mianyang are the top two cities in terms of GDP volume in Sichuan Province, which implies higher anthropogenic emission levels than other cities.

The multiyear average PM<sub>2.5</sub> concentration showed a close relationship with atmospheric diffusion ability (**Figure 9**). Taking Chengdu and Chongqing as examples, **Figure 10** shows that the interannual air quality changed with diffusion conditions. Monthly PM<sub>2.5</sub> concentrations exhibited a significant decreasing trend in Chengdu and Chongqing from the winter

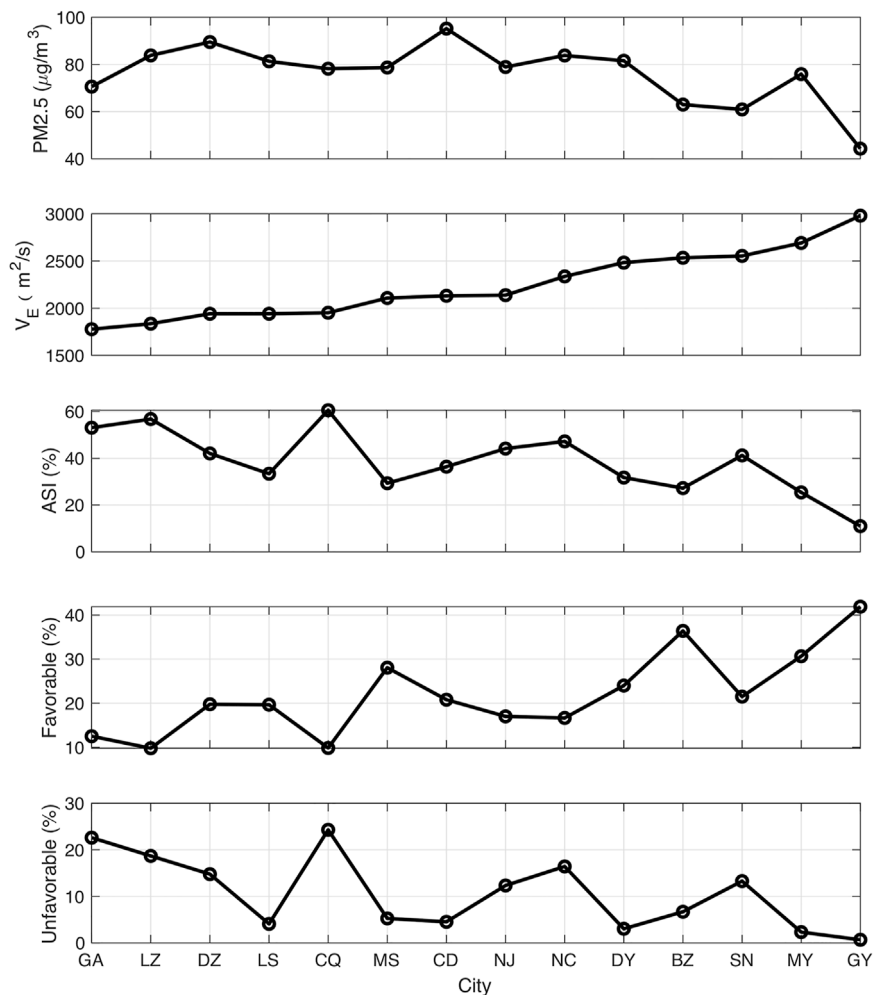


**FIGURE 9** | Variation of winter average PM2.5 concentrations with  $V_E$ , frequency of ASI, and favorable and unfavorable conditions in the 14 cities in the basin. All the variables are the average values during the winters from 2013 to 2019. Cities are ranked by the value of  $V_E$ .

of 2013–2019, with negative tendencies of  $-11.34$  and  $-8.93 \mu\text{g}/(\text{m}^3 \cdot \text{yr})$ . Based on the national air quality standard in China, daily mean PM2.5 concentrations lower than  $35 \mu\text{g}/\text{m}^3$  are good air quality days. **Figure 10** also shows the monthly occurrence of good air quality in the two cities from 2013 to 2019, showing significant increases of 2.12 and 2.87%/yr. The remarkable decrease in PM2.5 concentration and increase in the frequency of good air quality represent the success of emission reduction policies in recent years. The industrial and residential emissions of  $\text{SO}_2$  in Sichuan Province and Chongqing municipality decreased from  $1.29 \times 10^6$  to  $8.4 \times 10^5$  tons from 2011 to 2017, which contributed to the significant decrease in regional PM2.5 concentrations (National Bureau of Statistics of China, 2020). To exclude the effects of emission reduction on air quality, the detrending time series of PM2.5 concentration and frequency of good air quality were used to investigate the influence of atmospheric diffusion conditions on the interannual variation in air quality. There were significant correlations between the occurrence of good air quality and  $V_E$ /ASI/favorable

conditions in the two cities, with correlation coefficients of  $0.71/-0.5/0.6$  and  $0.47/-0.58/0.45$  in Chengdu and Chongqing, respectively. In addition, the PM2.5 concentration was significantly negatively correlated with  $V_E$  and favorable condition frequency in Chengdu. Moreover, **Table 1** summarizes the correlation coefficients between the metrics indicating atmospheric diffusion conditions and the series of “moderate,” “unhealthy for sensitive groups to unhealthy,” “very unhealthy to hazardous” air quality in Chengdu and Chongqing. Only the occurrence of good or very unhealthy to hazardous air quality was closely associated with atmospheric diffusion. The frequencies of occurrence of moderate to unhealthy air quality were insensitive to variations in ambient atmospheric conditions.

## 4 CONCLUSIONS AND DISCUSSION

Atmospheric diffusion controls the day-to-day evolution of air pollution episodes, the long-term variation of which has

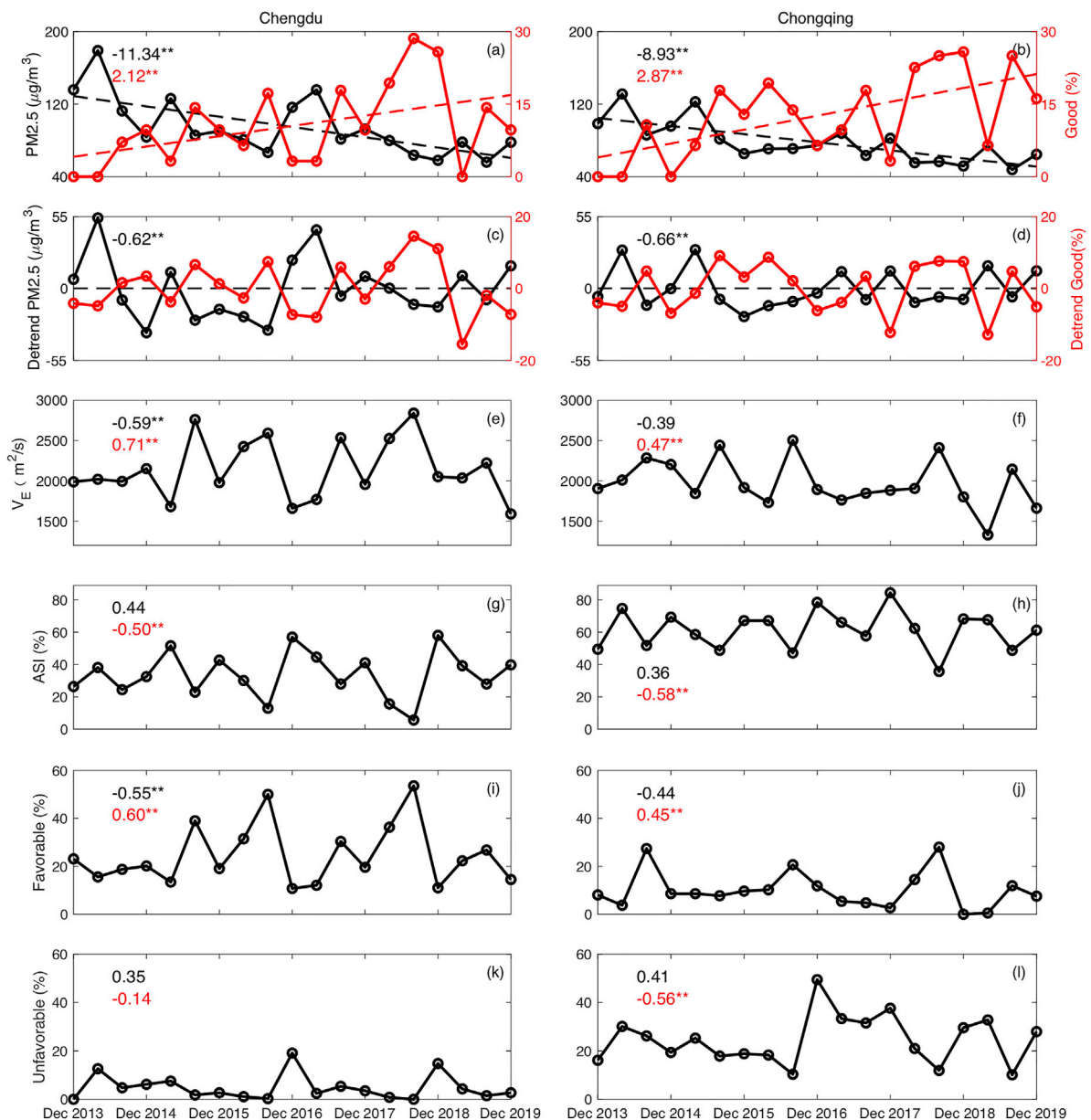


**FIGURE 10 |** Variation in monthly PM2.5 concentrations and good air quality frequency (A–B), detrending PM2.5 concentrations and good air quality frequency (C–D),  $V_E$  (E–F), frequencies of ASI (G–H), favorable (I–J) and unfavorable (K–L) conditions during the winters from 2013 to 2019 (19 months in total) in Chengdu and Chongqing. Detrending series were calculated by subtracting the linear trend from the original series. Values in Figs (A–B) are the linear trend of PM2.5 concentration (black) and good air quality (red). \*\* indicates significance at 0.01 of the linear trends based on least square method. Values in Figs (C–D) indicate the correlation coefficient of detrended PM2.5 concentrations and good air quality frequency. \*\* indicates that the correlation coefficient is significant at the 0.01 probability level. Values in Figs. (E–L) indicate the correlation coefficients between the detrended PM2.5 concentrations (black) and good air quality frequency (red) with the specific metric of atmospheric diffusion conditions. \*\* indicates that the correlation coefficient is significant at the 0.01 probability level.

important significance for the quantitative evaluation of historical emission reduction effects or the development of emission reduction measures. The spatial and temporal distributions of wintertime atmospheric diffusion conditions in the Sichuan Basin are examined in this work. The thresholds for occurrence of air stagnation events are established based on the relationship between PM2.5 concentrations and surface wind speed and potential temperature differences at 925 hPa and 800 hPa.  $V_E$

and the frequency of air stagnation events were incorporated to evaluate the variation in atmospheric diffusion conditions and their effects on air quality in the Sichuan Basin. Both atmospheric horizontal and vertical diffusion conditions are contained in the definitions of  $V_E$  and air stagnation events. Wind<sub>BL</sub>/BLH/Wind<sub>10</sub>/ $\Delta\theta$ , which are four independent variables, were used to indicate the capacity for horizontal and vertical diffusion ability, respectively. In terms of the spatial distribution of

**TABLE 1** | Correlation coefficients between the detrend PM<sub>2.5</sub> concentrations and the frequencies of different air quality levels with the specific metric indicating atmospheric diffusion conditions during the winter of 2013–2019 in Chengdu and Chongqing (\* indicates that the correlation coefficient is significant at the 0.01 probability level).

Chengdu/Chongqing	Monthly mean	Good	Moderate	Unhealthy for sensitive groups to unhealthy	Very unhealthy to hazardous
PM <sub>2.5</sub> (μg/m <sup>3</sup> )	—	0–35	35–75	75–115	>115
V <sub>E</sub>	-0.59*/-0.39	0.71*/0.48*	0.29/0.12	0.07/-0.07	-0.63*/-0.27
ASI	0.44/0.36	-0.5*/-0.58*	-0.15/-0.03	-0.31/0.09	0.54*/0.26
Favorable	-0.55*/-0.44	0.6*/0.46*	0.24/0.35	0.19/-0.20	-0.59*/-0.34
Unfavorable	0.35/0.41	-0.14/-0.56*	-0.26/-0.12	-0.34/0.15	0.47*/0.27

atmospheric diffusion conditions, V<sub>E</sub> exhibited a decreasing tendency from the northwest of the basin to its southeast, with the highest V<sub>E</sub> being higher than 3,400 m<sup>2</sup>/s compared to the lowest value of approximately 1,600 m<sup>2</sup>/s. The distribution of air stagnation event frequency is opposite to that of V<sub>E</sub>, showing a low frequency of approximately 15% over the northwestern high-altitude basin and a higher frequency of 60% over the southeastern low-altitude region. The northwest-southeast decrease in atmospheric diffusion conditions is attributed to the consistent spatial distribution of horizontal diffusion conditions and vertical conditions, both of which showed higher ability over the northwestern basin and lower ability over the southeast. The frequency of favorable conditions showed with a spatial distribution similar to that of V<sub>E</sub>, and the spatial variation in unfavorable conditions resembled that of air stagnation events.

Given the long-term variations in winter atmospheric diffusion conditions, V<sub>E</sub> showed a broadly increasing trend from 1979 to 2019, with a distinct increase in the western region and a weak negative trend in the eastern basin. The significant increase in BLH explained the positive tendency of V<sub>E</sub> over most of the basin, and the remarkable decrease in Wind<sub>BL</sub> drove the negative tendency of V<sub>E</sub> in the eastern basin. In contrast, the occurrence of air stagnation events showed a decreasing trend of ~3–6%/decade in the basin, which was more significant over the western part of the basin than over the eastern region. The decreasing pattern of ASI frequency was driven by the negative tendency of Δθ. Generally, both increasing V<sub>E</sub> and decreasing ASI frequency indicate the improvement of atmospheric diffusion conditions in the Sichuan Basin from 1979 to 2019, mitigating the effects of air pollutant emissions to some extent. The enhancement of atmospheric diffusion conditions is attributed to the improvement of vertical diffusion conditions (i.e., higher BLH and weaker Δθ). The recent better atmospheric diffusion conditions are also reflected by the significant increasing trend of favorable conditions over the western part of the basin, and the dramatic decrease in the unfavorable condition frequency over the eastern region.

Seasonal PM<sub>2.5</sub> concentrations declined with increasing local atmospheric diffusion conditions, with the best air quality in the northwest city of Guangyuan. Air quality in Chengdu and Mianyang were worse than in other cities with the same level of atmospheric diffusion conditions, perhaps because of their higher anthropogenic emission levels. The atmospheric diffusion

conditions showed significant correlations with the occurrence of “good” and “very unhealthy to hazardous” air quality, and the occurrence frequencies of “moderate” to “unhealthy” air quality were insensitive to the variation in ambient atmospheric conditions. Atmospheric diffusion conditions were able to explain approximately 25–50% of the interannual variation in PM<sub>2.5</sub> concentrations in Chengdu.

Long-term variation of daytime BLH have been investigated in many other studies, which shows remarkable increase trend over the past decades (Guo et al., 2016; Wang and Wang, 2016). The variation in wind speed, low tropospheric stability, surface temperature and cloud cover are considered as the dominant factors for the increase of BLH (Li et al., 2021; Guo et al., 2021). Considering the severe air pollution in the winter and poor performance of the stable BLH simulation, spatial and temporal variations in wintertime atmospheric diffusion conditions at 14:00 LST were investigated in this study. However, there were remarkable seasonal and diurnal differences in the processes in the atmospheric boundary layer (Stull, 2012; Wang and Wang, 2016), which may affect the variation in atmospheric diffusion conditions and warrant future studies.

## DATA AVAILABILITY STATEMENT

The original contributions presented in the study are included in the article/**Supplementary Material**, further inquiries can be directed to the corresponding author.

## AUTHOR CONTRIBUTIONS

GW and BC designed and conducted the research and analysis. WL and SJ collected data and contributed to the definition of air stagnation. GW, SJ and BC worked together on the interpretation of results and wrote the paper.

## FUNDING

This study was funded by the National Natural Science Foundation of China (41975075, 42075058 and 41805117) and Shanghai International Science and Technology Partnership Project (No. 21230780200).

## ACKNOWLEDGMENTS

Hourly PM<sub>2.5</sub> real-time data in China were downloaded from the website of Ministry of Ecology and Environment of the People's Republic of China (<http://106.37.208.233:20035>). The fifth generation European Centre for Medium-Range Weather Forecasts atmospheric reanalysis data (ECMWF ERA5) at 97–114°E and 25–35°N with a horizontal resolution of 0.25° × 0.25° from 1979 to 2019 are

downloaded from <https://www.ecmwf.int/en/forecasts/datasets/reanalysis-datasets/era5>.

## REFERENCES

- Bi, J., Huang, J., Holben, B., and Zhang, G. (2016). Comparison of Key Absorption and Optical Properties between Pure and Transported Anthropogenic Dust over East and Central Asia. *Atmos. Chem. Phys.* 16 (24), 15501–15516. doi:10.5194/acp-16-15501-2016
- Cai, W., Li, K., Liao, H., Wang, H., and Wu, L. (2017). Weather Conditions Conducive to Beijing Severe Haze More Frequent under Climate Change. *Nat. Clim. Change* 7 (4), 257–262. doi:10.1038/nclimate3249
- Cao, B., Wang, X., Ning, G., Yuan, L., Jiang, M., Zhang, X., et al. (2020). Factors Influencing the Boundary Layer Height and Their Relationship with Air Quality in the Sichuan Basin, China. *Sci. Total Environ.* 727, 138584. doi:10.1016/j.scitotenv.2020.138584
- Chang, L., Wu, Z., and Xu, J. (2020). Potential Impacts of the Southern Hemisphere Polar Vortices on central-eastern China Haze Pollution during Boreal Early winter. *Clim. Dyn.* 55 (3), 771–787. doi:10.1007/s00382-020-05294-3
- Che, H., Xia, X., Zhao, H., Dubovik, O., Holben, B. N., Goloub, P., et al. (2019). Spatial Distribution of Aerosol Microphysical and Optical Properties and Direct Radiative Effect from the China Aerosol Remote Sensing Network. *Atmos. Chem. Phys.* 19 (18), 11843–11864. doi:10.5194/acp-19-11843-2019
- Chen, H., and Wang, H. (2015). Haze Days in North China and the Associated Atmospheric Circulations Based on Daily Visibility Data from 1960 to 2012. *J. Geophys. Res. Atmos.* 120 (12), 5895–5909. doi:10.1002/2015jd023225
- Chen, H., Wang, H., Sun, J., Xu, Y., and Yin, Z. (2019a). Anthropogenic fine Particulate Matter Pollution Will Be Exacerbated in Eastern China Due to 21st century GHG Warming. *Atmos. Chem. Phys.* 19 (1), 233–243. doi:10.5194/acp-19-233-2019
- Chen, J., Li, Z., Lv, M., Wang, Y., Wang, W., Zhang, Y., et al. (2018). Aerosol Hygroscopic Growth, Contributing Factors and Impact On Haze Events in a Severely Polluted Region in Northern China. *Atmos. Chem. Phys.* 19 (2), 1327–1342. doi:10.5194/acp-19-1327-2019
- Chen, S., Zhang, X., Lin, J., Huang, J., Zhao, D., Yuan, T., et al. (2019b). Fugitive Road Dust PM<sub>2.5</sub> Emissions and Their Potential Health Impacts. *Environ. Sci. Technol.* 53 (14), 8455–8465. doi:10.1021/acs.est.9b00666
- Chen, Z., Chen, D., Zhao, C., Kwan, M.-p., Cai, J., Zhuang, Y., et al. (2020). Influence of Meteorological Conditions on PM<sub>2.5</sub> Concentrations across China: A Review of Methodology and Mechanism. *Environ. Int.* 139, 105558. doi:10.1016/j.envint.2020.105558
- Dang, R., and Liao, H. (2019). Severe winter Haze Days in the Beijing-Tianjin-Hebei Region from 1985 to 2017 and the Roles of Anthropogenic Emissions and Meteorology. *Atmos. Chem. Phys.* 19 (16), 10801–10816. doi:10.5194/acp-19-10801-2019
- Ding, A., Huang, X., Nie, W., Chi, X., Xu, Z., Zheng, L., et al. (2019). Significant Reduction of PM<sub>2.5</sub> in Eastern China Due to Regional-Scale Emission Control: Evidence from SORPES in 2011–2018. *Atmos. Chem. Phys.* 19 (18), 11791–11801. doi:10.5194/acp-19-11791-2019
- Fan, H., Zhao, C., and Yang, Y. (2020). A Comprehensive Analysis of the Spatio-Temporal Variation of Urban Air Pollution in China during 2014–2018. *Atmos. Environ.* 220, 117066. doi:10.1016/j.atmosenv.2019.117066
- Fan, J., Rosenfeld, D., Yang, Y., Zhao, C., Leung, L. R., and Li, Z. (2015). Substantial Contribution of Anthropogenic Air Pollution to Catastrophic Floods in Southwest China. *Geophys. Res. Lett.* 42 (14), 6066–6075. doi:10.1002/2015gl064479

## SUPPLEMENTARY MATERIAL

The Supplementary Material for this article can be found online at: <https://www.frontiersin.org/articles/10.3389/fenvs.2021.763504/full#supplementary-material>

- Feng, F., and Wang, K. (2019). Determining Factors of Monthly to Decadal Variability in Surface Solar Radiation in China: Evidences from Current Reanalyses. *J. Geophys. Res. Atmos.* 124 (16), 9161–9182. doi:10.1029/2018jd030214
- Gui, K., Che, H., Wang, Y., Wang, H., Zhang, L., Zhao, H., et al. (2019). Satellite-derived PM<sub>2.5</sub> Concentration Trends over Eastern China from 1998 to 2016: Relationships to Emissions and Meteorological Parameters. *Environ. Pollut.* 247, 1125–1133. doi:10.1016/j.envpol.2019.01.056
- Guo, J., Miao, Y., Zhang, Y., Liu, H., Li, Z., Zhang, W., et al. (2016). The Climatology of Planetary Boundary Layer Height in China Derived from Radiosonde and Reanalysis Data. *Atmos. Chem. Phys.* 16 (20), 13309–13319. doi:10.5194/acp-16-13309-2016
- Guo, J., Xu, H., Liu, L., Chen, D., Peng, Y., Yim, S. H. L., et al. (2019). The Trend Reversal of Dust Aerosol over East Asia and the North Pacific Ocean Attributed to Large-Scale Meteorology, Deposition, and Soil Moisture. *J. Geophys. Res. Atmos.* 124 (19), 10450–10466. doi:10.1029/2019jd030654
- Guo, J., Zhang, J., Yang, K., Liao, H., Zhang, S., Huang, K., et al. (2021). Investigation of Near-Global Daytime Boundary Layer Height Using High-Resolution Radiosondes: First Results and Comparison with ERA-5, MERRA-2, JRA-55, and NCEP-2 Reanalyses. *Atmos. Chem. Phys. Discuss.* [in review]. doi:10.5194/acp-2021-257
- He, J., Lu, S., Yu, Y., Gong, S., Zhao, S., and Zhou, C. (2018a). Numerical Simulation Study of winter Pollutant Transport Characteristics over Lanzhou City, Northwest China. *Atmosphere* 9 (10), 382. doi:10.3390/atmos9100382
- He, Y., Wang, K., Zhou, C., and Wild, M. (2018b). A Revisit of Global Dimming and Brightening Based on the sunshine Duration. *Geophys. Res. Lett.* 45 (9), 4281–4289. doi:10.1029/2018gl077424
- Hu, Z., Huang, J., Zhao, C., Ma, Y., Jin, Q., Qian, Y., et al. (2019). Trans-Pacific Transport and Evolution of Aerosols: Spatiotemporal Characteristics and Source Contributions. *Atmos. Chem. Phys.* 19, 12709–12730. doi:10.5194/acp-19-12709-2019
- Hu, Z., Jin, Q., Ma, Y., Pu, B., Ji, Z., Wang, Y., et al. (2021). Temporal Evolution of Aerosols and Their Extreme Events in Polluted Asian Regions during Terra's 20-year Observations. *Remote Sensing Environ.* 263, 112541. doi:10.1016/j.rse.2021.112541
- Huang, X., Wang, Z., and Ding, A. (2018). Impact of Aerosol-PBL Interaction on Haze Pollution: Multiyear Observational Evidences in North China. *Geophys. Res. Lett.* 45 (16), 8596–8603. doi:10.1029/2018gl079239
- Jian, B., Li, J., Wang, G., He, Y., Han, Y., Zhang, M., et al. (2018). The Impacts of Atmospheric and Surface Parameters on Long-Term Variations in the Planetary Albedo. *J. Clim.* 31 (21), 8705–8718. doi:10.1175/jcli-d-17-0848.1
- Li, J., Liao, H., Hu, J., and Li, N. (2019). Severe Particulate Pollution Days in China during 2013–2018 and the Associated Typical Weather Patterns in Beijing-Tianjin-Hebei and the Yangtze River Delta Regions. *Environ. Pollut.* 248, 74–81. doi:10.1016/j.envpol.2019.01.124
- Li, Q., Zhang, R., and Wang, Y. (2016). Interannual Variation of the Wintertime Fog-Haze Days across central and Eastern China and its Relation with East Asian winter Monsoon. *Int. J. Climatol.* 36 (1), 346–354. doi:10.1002/joc.4350
- Li, Y., Li, J., Zhao, Y., Lei, M., Zhao, Y., Jian, B., et al. (2021). Long-term Variation of Boundary Layer Height and Possible Contribution Factors: A Global Analysis. *Sci. Total Environ.* 796, 148950. doi:10.1016/j.scitotenv.2021.148950
- Liao, T., Gui, K., Jiang, W., Wang, S., Wang, B., Zeng, Z., et al. (2018). Air Stagnation and its Impact on Air Quality during winter in Sichuan and Chongqing, Southwestern China. *Sci. Total Environ.* 635, 576–585. doi:10.1016/j.scitotenv.2018.04.122

- Liu, Y., Tang, G., Huang, X., Wei, K., Wu, S., Wang, M., et al. (2021). Unexpected Deep Mixing Layer in the Sichuan Basin, China. *Atmos. Res.* 249, 105300. doi:10.1016/j.atmosres.2020.105300
- Liu, Y., Tang, G., Zhou, L., Hu, B., Liu, B., Li, Y., et al. (2019). Mixing Layer Transport Flux of Particulate Matter in Beijing, China. *Atmos. Chem. Phys.* 19 (14), 9531–9540. doi:10.5194/acp-19-9531-2019
- Lu, C., Deng, Q.-h., Liu, W.-w., Huang, B.-l., and Shi, L.-z. (2012). Characteristics of Ventilation Coefficient and its Impact on Urban Air Pollution. *J. Cent. South. Univ. Technol.* 19 (3), 615–622. doi:10.1007/s11771-012-1047-9
- Ma, Y., Ye, J., Xin, J., Zhang, W., Vilà-Guerau de Arellano, J., Wang, S., et al. (2020). The Stove, Dome, and Umbrella Effects of Atmospheric Aerosol on the Development of the Planetary Boundary Layer in Hazy Regions. *Geophys. Res. Lett.* 47 (13). doi:10.1029/2020gl087373
- Miao, Y., Guo, J., Liu, S., Liu, H., Li, Z., Zhang, W., et al. (2017). Classification of Summertime Synoptic Patterns in Beijing and Their Associations with Boundary Layer Structure Affecting Aerosol Pollution. *Atmos. Chem. Phys.* 17 (4), 3097–3110. doi:10.5194/acp-17-3097-2017
- Mu, M., and Zhang, R. (2014). Addressing the Issue of Fog and Haze: A Promising Perspective from Meteorological Science and Technology. *Sci. China Earth Sci.* 57, 1–2. doi:10.1007/s11430-013-4791-2
- National Bureau of Statistics of China (2020). <https://data.stats.gov.cn/easyquery.htm?cn=C01>. Accessed November 3, 2021.
- Ning, G., Wang, S., Ma, M., Ni, C., Shang, Z., Wang, J., et al. (2018). Characteristics of Air Pollution in Different Zones of Sichuan Basin, China. *Sci. Total Environ.* 612, 975–984. doi:10.1016/j.scitotenv.2017.08.205
- Ning, G., Yim, S. H. L., Wang, S., Duan, B., Nie, C., Yang, X., et al. (2019). Synergistic Effects of Synoptic Weather Patterns and Topography on Air Quality: a Case of the Sichuan Basin of China. *Clim. Dyn.* 53 (11), 6729–6744. doi:10.1007/s00382-019-04954-3
- Stull, R. B. (2012). *An Introduction to Boundary Layer Meteorology*. Dordrecht: Springer Science & Business Media.
- Sujatha, P., Mahalakshmi, D. V., Ramiz, A., Rao, P. V. N., and Naidu, C. V. (2016). Ventilation Coefficient and Boundary Layer Height Impact on Urban Air Quality. *Cogent Environ. Sci.* 2 (1), 1125284. doi:10.1080/23311843.2015.1125284
- Sun, Y. L., Wang, Z. F., Fu, P. Q., Yang, T., Jiang, Q., Dong, H. B., et al. (2013). Aerosol Composition, Sources and Processes during Wintertime in Beijing, China. *Atmos. Chem. Phys.* 13 (9), 4577–4592. doi:10.5194/acp-13-4577-2013
- Tang, G., Zhu, X., Hu, B., Xin, J., Wang, L., Münkel, C., et al. (2015). Impact of Emission Controls on Air Quality in Beijing during APEC 2014: Lidar Ceilometer Observations. *Atmos. Chem. Phys.* 15 (21), 12667–12680. doi:10.5194/acp-15-12667-2015
- Wang, K., Dickinson, R. E., and Liang, S. (2009). Clear Sky Visibility Has Decreased over Land Globally from 1973 to 2007. *Science* 323 (5920), 1468–1470. doi:10.1126/science.1167549
- Wang, L., and Wang, K. (2015). Impacts of DEM Uncertainty on Estimated Surface Solar Radiation and Extracted River Network. *Bull. Am. Meteorol. Soc.* 96 (2), 297–304. doi:10.1175/bams-d-13-00285.1
- Wang, X., Dickinson, R. E., Su, L., Zhou, C., and Wang, K. (2018a). PM<sub>2.5</sub> Pollution in China and How it Has Been Exacerbated by Terrain and Meteorological Conditions. *Bull. Am. Meteorol. Soc.* 99 (1), 105–119. doi:10.1175/bams-d-16-0301.1
- Wang, X., and Wang, K. (2016). Homogenized Variability of Radiosonde-Derived Atmospheric Boundary Layer Height over the Global Land Surface from 1973 to 2014. *J. Clim.* 29 (19), 6893–6908. doi:10.1175/jcli-d-15-0766.1
- Wang, X., Wang, K., and Su, L. (2016). Contribution of Atmospheric Diffusion Conditions to the Recent Improvement in Air Quality in China. *Sci. Rep.* 6, 36404. doi:10.1038/srep36404
- Wang, X., Wen, H., Shi, J., Bi, J., Huang, Z., Zhang, B., et al. (2018b). Optical and Microphysical Properties of Natural mineral Dust and Anthropogenic Soil Dust Near Dust Source Regions over Northwestern China. *Atmos. Chem. Phys.* 18 (3), 2119–2138. doi:10.5194/acp-18-2119-2018
- Wang, X., and Zhang, R. (2020a). Effects of Atmospheric Circulations on the Interannual Variation in PM<sub>2.5</sub> Concentrations over the Beijing-Tianjin-Hebei Region in 2013–2018. *Atmos. Chem. Phys.* 20 (13), 7667–7682. doi:10.5194/acp-20-7667-2020
- Wang, X., and Zhang, R. (2020b). How Did Air Pollution Change during the COVID-19 Outbreak in China. *Bull. Am. Meteorol. Soc.* 101 (10), E1645–E1652. doi:10.1175/bams-d-20-0102.1
- Wang, Y., Meng, Z., Lyu, R., Huang, G., He, Q., and Cheng, T. (2020). Spatiotemporal Changes of Surface Solar Radiation: Implication for Air Pollution and rice Yield in East China. *Sci. Total Environ.* 739, 140361. doi:10.1016/j.scitotenv.2020.140361
- Xia, X., Che, H., Shi, H., Chen, H., Zhang, X., Wang, P., et al. (2020). Advances in Sunphotometer-Measured Aerosol Optical Properties and Related Topics in China: Impetus and Perspectives. *Atmos. Res.* 249, 105286. doi:10.1016/j.atmosres.2020.105286
- Yin, Z., Wang, H., and Chen, H. (2017). Understanding Severe winter Haze Events in the North China Plain in 2014: Roles of Climate Anomalies. *Atmos. Chem. Phys.* 17 (3), 1641–1651. doi:10.5194/acp-17-1641-2017
- Zhang, L., Guo, X., Zhao, T., Gong, S., Xu, X., Li, Y., et al. (2019). A Modelling Study of the Terrain Effects on Haze Pollution in the Sichuan Basin. *Atmos. Environ.* 196, 77–85. doi:10.1016/j.atmosenv.2018.10.007
- Zhang, Q., and Geng, G. (2019). Impact of Clean Air Action on PM<sub>2.5</sub> Pollution in China. *Sci. China Earth Sci.* 62, 1845–1846. doi:10.1007/s11430-019-9531-4
- Zhang, R., Li, Q., and Zhang, R. (2014). Meteorological Conditions for the Persistent Severe Fog and Haze Event over Eastern China in January 2013. *Sci. China Earth Sci.* 57 (1), 26–35. doi:10.1007/s11430-013-4774-3
- Zhang, R. (2017). Warming Boosts Air Pollution. *Nat. Clim Change* 7 (4), 238–239. doi:10.1038/nclimate3257
- Zhao, C., and Garrett, T. J. (2015). Effects of Arctic Haze on Surface Cloud Radiative Forcing. *Geophys. Res. Lett.* 42 (2), 557–564. doi:10.1002/2014gl062015
- Zhao, C., Li, Y., Zhang, F., Sun, Y., and Wang, P. (2018a). Growth Rates of fine Aerosol Particles at a Site Near Beijing in June 2013. *Adv. Atmos. Sci.* 35 (2), 209–217. doi:10.1007/s00376-017-7069-3
- Zhao, D., Schmitt, S. H., Wang, M., Acir, I.-H., Tillmann, R., Tan, Z., et al. (2018b). Effects of NO<sub>x</sub> and SO<sub>2</sub> on the Secondary Organic Aerosol Formation from Photooxidation of  $\alpha$ -pinene and Limonene. *Atmos. Chem. Phys.* 18, 1611–1628. doi:10.5194/acp-18-1611-2018
- Zhao, H., Che, H., Zhang, L., Gui, K., Ma, Y., Wang, Y., et al. (2020). How Aerosol Transport from the North China plain Contributes to Air Quality in Northeast China. *Sci. Total Environ.* 738, 139555. doi:10.1016/j.scitotenv.2020.139555
- Zhao, S., Yu, Y., Yin, D., Qin, D., He, J., and Dong, L. (2018c). Spatial Patterns and Temporal Variations of Six Criteria Air Pollutants during 2015 to 2017 in the City Clusters of Sichuan Basin, China. *Sci. total Environ.* 624, 540–557. doi:10.1016/j.scitotenv.2017.12.172
- Zhong, J., Zhang, X., Wang, Y., Wang, J., Shen, X., Zhang, H., et al. (2019). The Two-Way Feedback Mechanism between Unfavorable Meteorological Conditions and Cumulative Aerosol Pollution in Various Haze Regions of China. *Atmos. Chem. Phys.* 19 (5), 3287–3306. doi:10.5194/acp-19-3287-2019
- Zhu, X., Tang, G., Guo, J., Hu, B., Song, T., Wang, L., et al. (2018). Mixing Layer Height on the North China Plain and Meteorological Evidence of Serious Air Pollution in Southern Hebei. *Atmos. Chem. Phys.* 18 (7), 4897–4910. doi:10.5194/acp-18-4897-2018

**Conflict of Interest:** The authors declare that the research was conducted in the absence of any commercial or financial relationships that could be construed as a potential conflict of interest.

**Publisher's Note:** All claims expressed in this article are solely those of the authors and do not necessarily represent those of their affiliated organizations, or those of the publisher, the editors and the reviewers. Any product that may be evaluated in this article, or claim that may be made by its manufacturer, is not guaranteed or endorsed by the publisher.

Copyright © 2021 Wang, Leng, Jiang and Cao. This is an open-access article distributed under the terms of the Creative Commons Attribution License (CC BY). The use, distribution or reproduction in other forums is permitted, provided the original author(s) and the copyright owner(s) are credited and that the original publication in this journal is cited, in accordance with accepted academic practice. No use, distribution or reproduction is permitted which does not comply with these terms.